



Universiteit  
Leiden  
The Netherlands

## **Long-term imaging reveals a circadian rhythm of intracellular chloride in neurons of the suprachiasmatic nucleus**

Klett, N.J.; Cravetchi, O.; Allen, C.N.

### **Citation**

Klett, N. J., Cravetchi, O., & Allen, C. N. (2022). Long-term imaging reveals a circadian rhythm of intracellular chloride in neurons of the suprachiasmatic nucleus. *Journal Of Biological Rhythms*, 37(1), 110-123. doi:10.1177/07487304211059770

Version: Publisher's Version

License: [Leiden University Non-exclusive license](#)

Downloaded from: <https://hdl.handle.net/1887/3502475>

**Note:** To cite this publication please use the final published version (if applicable).

# Long-Term Imaging Reveals a Circadian Rhythm of Intracellular Chloride in Neurons of the Suprachiasmatic Nucleus

Nathan J. Klett<sup>\*,†,‡</sup> , Olga Cravetchi<sup>†</sup>, and Charles N. Allen<sup>†,§,1</sup> 

<sup>\*</sup>Neuroscience Graduate Program, Oregon Health & Science University, Portland, Oregon, USA,

<sup>†</sup>Oregon Institute for Occupational Health Sciences, Oregon Health & Science University,

Portland, Oregon, USA, <sup>‡</sup>Neurophysiology, Department of Cell and Chemical Biology,

Leiden University Medical Center, Leiden, The Netherlands, and <sup>§</sup>Department of Behavioral

Neuroscience, Oregon Health & Science University, Portland, Oregon, USA

**Abstract** Both inhibitory and excitatory GABA transmission exist in the mature suprachiasmatic nucleus (SCN), the master pacemaker of circadian physiology. Whether GABA is inhibitory or excitatory depends on the intracellular chloride concentration ( $[Cl^-]_i$ ). Here, using the genetically encoded ratiometric probe Cl-Sensor, we investigated  $[Cl^-]_i$  in AVP and VIP-expressing SCN neurons for several days in culture. The chloride ratio ( $R_{Cl}$ ) demonstrated circadian rhythmicity in AVP + neurons and VIP + neurons, but was not detected in GFAP + astrocytes.  $R_{Cl}$  peaked between ZT 7 and ZT 8 in both AVP + and VIP + neurons.  $R_{Cl}$  rhythmicity was not dependent on the activity of several transmembrane chloride carriers, action potential generation, or the L-type voltage-gated calcium channels, but was sensitive to GABA antagonists. We conclude that  $[Cl^-]_i$  is under circadian regulation in both AVP + and VIP + neurons.

**Keywords** GABA, suprachiasmatic nucleus, chloride, vasopressin, vasoactive intestinal peptide

The suprachiasmatic nucleus (SCN) of the anterior hypothalamus is the master circadian pacemaker in mammals. Although individual SCN neurons can function as cell-autonomous circadian pacemakers, the SCN neural network is essential for the generation of precise circadian output. SCN neurons are GABAergic, and recently it has been shown that a subset of intrinsically photosensitive retinal ganglion cells release GABA in the SCN (Sonoda et al., 2020). Within the SCN, GABA transmission regulates the

clock's response to light input as well as the strength of coupling between individual neurons (Moldavan et al., 2006; Gillespie et al., 1996, 1997; Liu and Reppert, 2000; Albus et al., 2005; Evans et al., 2013; Freeman et al., 2013; DeWoskin et al., 2015). While GABA is traditionally thought of as an inhibitory neurotransmitter, GABA transmission is excitatory during brain development (but see Valeeva et al., 2016) and in certain pathological states (Gamba, 2005; Blaesse et al., 2009; Ben-Ari et al., 2012). Furthermore,

1 To whom all correspondence should be addressed: Charles N. Allen, Department of Behavioral Neuroscience, Oregon Health & Science University, Mail Code L606, 3181 Southwest Sam Jackson Park Road, Portland, OR 97239-3098, USA; e-mail: allenc@ohsu.edu.

excitatory GABA transmission has been observed in several regions of the adult brain, including the SCN (Wagner et al., 1997, 2001; De Jeu and Pennartz, 2002; Albus et al., 2005; Choi et al., 2008; Irwin and Allen, 2009; Freeman et al., 2013; Alamilla et al., 2014; Farajnia et al., 2014; Fan et al., 2015; Myung et al., 2015). Although there is evidence to support a functional role for excitatory GABA transmission in encoding photoperiod (Rohr et al., 2019; Farajnia et al., 2014; Evans et al., 2013), the physiological role of excitatory GABA signaling in the SCN remains unclear.

Due to the GABA<sub>A</sub> receptor's permeability to Cl<sup>-</sup> and HCO<sub>3</sub><sup>-</sup> ions, whether GABA is depolarizing or hyperpolarizing depends, in part, on the intracellular chloride concentration ([Cl<sup>-</sup>]<sub>i</sub>). [Cl<sup>-</sup>]<sub>i</sub> is determined by the concerted activity of a family of cation chloride cotransporters (CCCs). Generally, the sodium-potassium-chloride cotransporter 1 (NKCC1), transports Cl<sup>-</sup> ions into neurons, while the potassium-chloride cotransporters (KCC) transport Cl<sup>-</sup> out of neurons (Blaesse et al., 2009). Interestingly, immunohistochemistry has shown differential expression of chloride transporters throughout the SCN (Belenky et al., 2010), suggesting that [Cl<sup>-</sup>]<sub>i</sub>, and therefore the GABAergic reversal potential, may vary regionally within the SCN (Klett and Allen, 2017). Over the last decade, several groups have verified the importance of the CCCs in regulating [Cl<sup>-</sup>]<sub>i</sub> in the SCN (Choi et al., 2008; Irwin and Allen, 2009; Alamilla et al., 2014; Farajnia et al., 2014; Klett and Allen, 2017; Olde Engberink et al., 2018).

In this report, we performed epifluorescent imaging of organotypic slice cultures to assess the circadian regulation of [Cl<sup>-</sup>]<sub>i</sub> in the SCN over the course of several days. To monitor [Cl<sup>-</sup>]<sub>i</sub>, we made use of the ratiometric chloride indicator, Cl-Sensor. Cl-Sensor is a fluorescent reporter composed of a Cl-sensitive YFP moiety linked to a Cl-insensitive CFP moiety (Batti et al., 2013; Markova et al., 2008). Obtaining the ratio of these two fluorescent signals (R<sub>Cl</sub>) allows one to estimate [Cl<sup>-</sup>]<sub>i</sub> in the physiological range. Compared to electrophysiological techniques, imaging offers the advantage of monitoring [Cl<sup>-</sup>]<sub>i</sub> from multiple cells simultaneously without disrupting the native cellular milieu. Using Cre-lox recombination techniques, we targeted Cl-Sensor to arginine vasopressin (AVP) or vasoactive intestinal peptide (VIP) expressing SCN neurons, as well as glial fibrillary acidic protein (GFAP) expressing astrocytes. Using these mice, we observed a circadian rhythm in both AVP + and VIP + SCN neurons that was not present in GFAP + astrocytes. Further, the R<sub>Cl</sub> rhythm of AVP + neurons was found to be sensitive to GABA antagonists.

## MATERIALS AND METHODS

### Animal Strains and Housing

Cl<sup>-</sup> imaging experiments were performed with C57BL/6 mice in which a floxed Cl-Sensor allele was inserted into the Rosa26 locus (Batti et al., 2013). We crossed these mice with either AVP-IRES-Cre (Harris et al., 2014), VIP-IRES-Cre (Taniguchi et al., 2011; Harris et al., 2014), or GFAP-Cre mice (B6.Cg-Tg(Gfap-cre)73.12Mvs/J; Jackson Laboratory) to yield AVP::Cl-Sensor, VIP::Cl-Sensor, or GFAP::Cl-Sensor mice. Tail snips were sent to an external facility for genotyping (Transnetyx, Inc). Mice were heterozygous for both the Cl-Sensor and Cre transgenes. Brain slices were prepared from adult male and female mice between 2 and 6 months old.

Mice were housed in an environmental chamber (Percival Scientific, Perry, IA) maintained at 20°C -21°C on a 12:12h light:dark cycle, with free access to food and water. Data are plotted in relation to the time of lights on (zeitgeber time or ZT, lights on = ZT 0). All procedures were approved in advance by the Animal Care and Use Committees of Oregon Health and Science University.

### Long Term Imaging of Cl-Sensor

Using sterile techniques, brains were quickly removed and submerged in chilled Hanks' buffered salt solution (HBSS). Cultures were prepared as described previously (Moldavan et al., 2017; Hablitz et al., 2020). Briefly, the brain was blocked and 150 μm coronal slices were prepared with a vibratome (Leica VT 1000S, Leica Biosystems GmbH, Nussloch, Germany). SCN slices were trimmed to remove surrounding hypothalamic tissue, and positioned unto Millipore Millicell cell culture inserts (Sigma-Aldrich, St. Louis, MO). Inserts were placed in 35 mm culture dishes containing 1.2 mL culture medium and sealed with vacuum grease. Culture medium consisted of DMEM (Sigma-Aldrich, St. Louis, MO Cat# D 2902) supplemented with B27 (Life Technologies, ThermoFisher Scientific), 20 mM glucose, 10 mM HEPES, 4.2 mM NaHCO<sub>3</sub>, 25 μg/mL penicillin, and 25 μg/mL streptomycin. pH was adjusted to 7.2 with NaOH. Dishes were sealed with vacuum grease, incubated for a period of 2 to 6 h and subsequently placed in a 37°C temperature-controlled chamber positioned on the stage of an inverted fluorescent microscope (ECLIPSE TE2000-U, Nikon, Tokyo, Japan). Excitation light was supplied by a xenon arc lamp, and excitation wavelength was controlled by a filter wheel (Lambda 10-3, Sutter Instrument, Novato, CA). Excitation of YFP at 500/20nm preceded excitation of

CFP at 436/20 nm to promote Cl-Sensor photostability (Friedel et al., 2013). Excitation duration was between 500 and 1000 milliseconds. Images were acquired at 10X (NA 0.30) every 5 or 10 min with a CFP/YFP filter set (Chroma, 51017, Bellow Falls, VT), a beamsplitter (Dual-View, Photometrics, Tucson, AZ) and an Evolve EMCCD camera (Photometrics, Tucson, AZ). Equipment control and image processing were performed with Metafluor software (Molecular Devices, Sunnyvale, CA). Regions of interest (ROI) were defined around groups of fluorescent neurons or single neurons on each side of the SCN, and a dim region of the field of view was selected as background. Background values were subtracted from ROI intensity values for each frame.

### Immunohistochemistry

Mice were anesthetized with isoflurane and transcardially perfused with 1X phosphate buffered saline (PBS, pH 7.4), followed by 4% paraformaldehyde (PFA) in PBS. After perfusion, the brain was left to incubate in PFA for 18 h at 4°C. Subsequently, the brain was cryoprotected with overnight incubation in 10% sucrose in PBS (first night) and 30% sucrose in PBS (second night). In preparation for sectioning, brain blocks were embedded in Shandon Cryochrome Embedding Medium (Thermo Fisher Scientific Inc.) and fast-frozen with a mixture of dry ice and 96% ethanol for 3–5 min. Coronal (20 µm thick) sections were cut with a Leica cryostat (CM1950, Leica Microsystems, Inc.), thaw-mounted onto pre-cleaned SuperFrost Plus glass slides, and dried at 37°C. Dry SCN-containing sections were then rehydrated in 0.1 M phosphate buffer (PB). To reduce background autofluorescence, the sections were incubated in an aldehyde-reducing agent (1% NaBH<sub>4</sub> in 0.1 M PB) for 30 min and rinsed with multiple changes of 0.1 M PB. The tissue was then permeabilized with 0.3% Triton X-100 in TBS and non-specific binding was blocked by incubation in 5% normal donkey serum for 1 h at room temperature. For GFAP staining, the primary antibody was mouse anti-GFAP (1:1000, Millipore Bioscience Research Reagents MAB 3402, RRID: AB\_94844). The secondary antibody was donkey anti-mouse Dy-Light 594 (1:1000, Jackson ImmunoResearch #715-585-151, RRID: AB\_2340855). The images were acquired using a Zeiss 780 confocal laser scanning microscope and processed with ImageJ.

### Drugs

Tetrodotoxin (TTX) was acquired from Affix Scientific (Fremont, CA) and stored in water at 2 mM.

Bumetanide, VU0240551, picrotoxin, nimodipine, and GABAzine (SR 95531 hydrobromide) were acquired from Tocris Bioscience (Bristol, United Kingdom). Bumetanide and picrotoxin were dissolved and stored in DMSO at 100 mM. VU0240551 was dissolved in DMSO at 20 mM. GABAzine stock was dissolved in water at 2 mM. The anion exchange blocker 4,4'-diisothiocyano-2,2'-stilbenedisulfonic acid (DIDS) was acquired from Sigma-Aldrich (St. Louis, MO) and stored in DMSO at 100 mM before use. Strychnine hydrochloride, diazepam, zolpidem, and 5-Nitro-2-(3-phenylpropylamino)benzoic acid (NPPB) were purchased from Sigma-Aldrich (St. Louis, MO).

### Statistics and Analysis

The ROI time-series data were uploaded into the Lumicycle Analysis Program (Actimetrics, Wilmette, IL). The data beginning at the first nadir and continuing for three full cycles were detrended using the program's 24 h rolling average baseline subtraction function. For Lomb-Scargle periodogram analysis, the detrended data were then loaded into the Lomb package (<https://CRAN.R-project.org/package=lomb>) running in R studio (Version 1.2.5033) (Ruf, 1999). Experiments in which the highest value of normalized peak power fell outside of the circadian range of 18 to 30 h were considered arrhythmic, and were excluded from subsequent analysis of period, phase, and power. Graphpad Prism (Version 8.4.2) was used for plotting and statistical analysis. Drugs were tested in AVP::Cl-Sensor SCN slices, and drug effects were compared to AVP + control experiments using an one-way ANOVA, while VIP + control experiments were compared to AVP + control experiments using the unpaired Student's *t*-test. Data are presented as the mean ± standard error.

## RESULTS

To examine whether [Cl<sup>-</sup>]<sub>i</sub> may be under circadian regulation, we performed long-term chloride imaging of SCN slice cultures. To drive Cl-Sensor expression, we used a Cre-inducible mouse line, with a floxed Cl-Sensor allele inserted into the Rosa26 locus (Batti et al., 2013). In order to obtain Cl-Sensor expression in the SCN, we crossed these mice with either AVP-IRES-Cre or VIP-IRES-Cre mice to give Cl-Sensor expression in either AVP + or VIP + SCN neurons (Taniguchi et al., 2011; Harris et al., 2014). The resultant AVP::Cl-Sensor mice displayed Cl-Sensor expression in the dorsomedial SCN, while the VIP::Cl-Sensor mice displayed Cl-Sensor expression in the

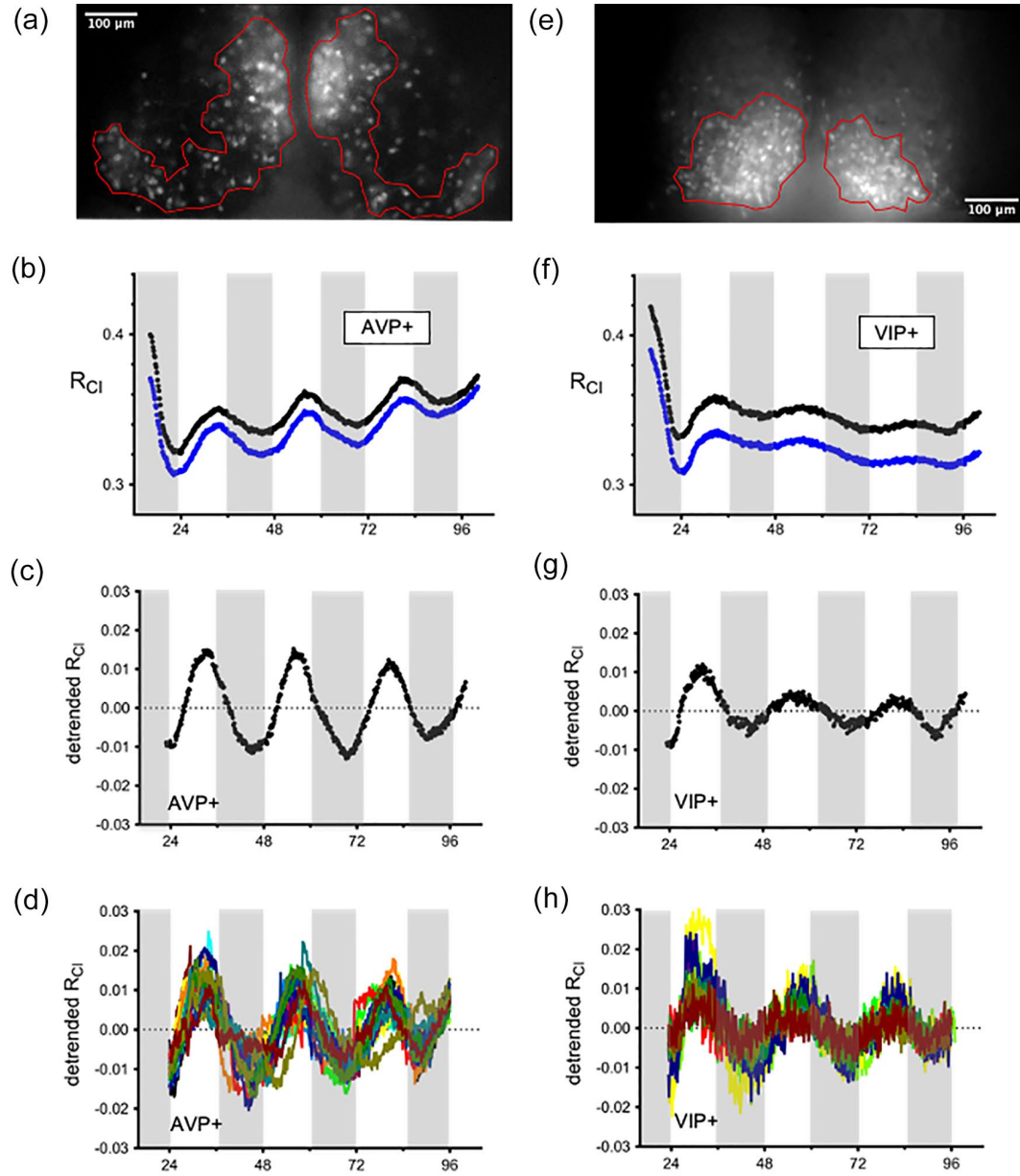


**Figure 1.** Long-term imaging of  $R_{Cl}$  from SCN explants. Fluorescent images of cultured SCN explants from an AVP::Cl-Sensor (a) or VIP::Cl-Sensor mouse (e). Regions of interest were defined around large groups of neurons in the left and right SCN. Raw values of  $R_{Cl}$  from the left (black trace) and right (blue trace) SCN of an AVP::Cl-Sensor (b) or VIP::Cl-Sensor mice (f). The periods of darkness during the animal's prior light/dark cycle are indicated with shading.  $R_{Cl}$  data from an AVP::Cl-Sensor mouse (c) or VIP::Cl-Sensor mouse (g) following detrending. Each trace represents a measure of  $R_{Cl}$  from a cluster of neurons in the left or right SCN.  $[Cl^-]_i$  is high during the day and peaks at approximately ZT 8. Rhythmicity could also be detected at the level of single cells in both AVP + (d) and VIP + (h) neurons. Abbreviations:  $R_{Cl}$ =chloride ratio; SCN=suprachiasmatic nucleus; AVP=arginine vasopressin; VIP=vasoactive intestinal peptide; ZT=zeitgeber time.

ventrolateral SCN, as expected for AVP and VIP expression (Figure 1a and 1e, van den Pol, 1986). Regions of interest were defined around clusters of neurons in the SCN slice. To obtain the chloride ratio ( $R_{Cl}$ ), we plotted the fluorescence emission from CFP excitation at 436nm over the emission from exciting

YFP<sub>Cl</sub> at 500 nm, so that an increase in  $R_{Cl}$  indicates an increase in  $[Cl^-]_i$ . Interestingly, we observed a circadian rhythm of  $R_{Cl}$  in AVP + neurons (8 out of 9 slices) that persisted for several days (Figure 1b). In order to extract circadian parameters from the data, it was necessary to detrend the traces (Figure 1c).  $R_{Cl}$  was



found to peak during midday, at approximately ZT 8 (ZT  $7.9 \pm 0.5$  h,  $n=8$  slices), indicating that  $[Cl^-]_i$  is high during the day, and low during the night. Following Lomb-Scargle periodogram analysis, we found that the  $R_{Cl}$  rhythm had a mean period of  $23.8 \pm 0.3$  h and an average normalized peak power of  $184.9 \pm 7.3$  ( $n=8$ ). Using VIP::Cl-Sensor mice, we observed that  $R_{Cl}$  also oscillated in VIP + neurons (8 out of 11 slices, Figure 1f and 1g). In VIP + neurons,  $R_{Cl}$  was found to peak around ZT 7 (ZT  $7.1 \pm 0.5$  h) and had an average period of  $23.2 \pm 0.6$  h ( $n=8$  slices). The time of peak was not significantly different between AVP + and VIP + neurons, but the amplitude of the first peak was found to be larger in AVP + neurons compared to VIP + neurons (Student's *t*-test,  $p=0.03$ , Figure 6b). Periodogram analysis revealed that the average normalized peak power was smaller in VIP + neurons ( $125.4 \pm 19.3$ ; Student's *t*-test,  $p=0.0121$ , Figure 6d), indicating that the rhythm was weaker in VIP + neurons compared to AVP + neurons. Rhythmicity could be detected within single cells for both AVP + (Figure 1d) and VIP + neurons (Figure 1h). These results indicate that  $[Cl^-]_i$  peaks during the day in both AVP + and VIP + SCN neurons.

We next asked whether the observed rhythmicity of  $R_{Cl}$  was specific to neurons, or could also be observed in SCN astrocytes. To obtain Cl-Sensor expression in astrocytes, we made use of a transgenic mouse line in which Cre expression is driven by the GFAP promoter. Crossing these mice with the floxed Cl-Sensor mice yielded GFAP::Cl-Sensor mice. Immunohistochemical analysis of these mice confirmed that Cl-Sensor is expressed in GFAP + astrocytes in the SCN (Figure 2a). From these GFAP::Cl-Sensor mice, we again prepared organotypic slice cultures of the SCN and defined a region of interest around the entire left SCN, but observed no rhythmicity in  $R_{Cl}$  ( $n=5$ ; Figure 2b), indicating that  $R_{Cl}$  rhythmicity is specific to SCN neurons.

We next tested whether the observed cycling of  $R_{Cl}$  may be due to CCC regulation of the intracellular chloride concentration. Indeed, previous studies have implicated these transporters in  $[Cl^-]_i$  regulation in SCN neurons (Choi et al., 2008; Irwin and Allen, 2009; Belenky et al., 2010; Farajnia et al., 2014; Klett and Allen, 2017; Alamilla et al., 2014; Rohr et al., 2019; Myung et al., 2015; McNeill et al., 2018; Olde Engberink et al., 2018). To test for the activity of CCCs in driving the rhythm in  $R_{Cl}$ , we cultured SCN slices from AVP::Cl-Sensor mice in the presence of antagonists to the CCCs. We used a high concentration of the non-selective CCC inhibitor bumetanide (100  $\mu$ M), as well as 20  $\mu$ M of VU0240551, which selectively targets the KCC family of chloride transporters (Delpire et al., 2009). However, we observed that  $R_{Cl}$

cycling persisted in the presence of these drugs, indicating that the CCCs do not drive the rhythmicity in  $R_{Cl}$  (average period =  $23.4 \pm 0.3$  h; average normalized peak power =  $189.1 \pm 15.9$ ;  $n=3$  slices; Figure 3a). Neuronal  $[Cl^-]_i$  is also regulated by the anion exchangers (Farrant and Kaila, 2007). To test if anion exchangers underlie the rhythm in  $R_{Cl}$ , we cultured SCN slices from an AVP::Cl-Sensor mice in the presence of the anion exchange inhibitor DIDS. However,  $R_{Cl}$  rhythmicity was not perturbed in the presence of 100  $\mu$ M DIDS (average period =  $23.8 \pm 0.4$  h; average normalized peak power =  $203.5 \pm 14.3$ ;  $n=3$  slices; Figure 3b). Recently, the expression of the calcium-activated chloride channel (CaCC) anoctamin-1 has been demonstrated in the SCN (Aguilar-Roblero et al., 2018). To investigate whether anoctamin-1 drives the rhythm in  $R_{Cl}$ , we targeted the CaCCs with the blocker 5-nitro-2-(3-phenylpropylamino) benzoic acid (NPPB) (Jeon et al., 2013; Huang et al., 2012; Berg et al., 2012).  $R_{Cl}$  rhythmicity persisted when SCN slices were cultured in the presence of NPPB (average period =  $23.5 \pm 0.2$  h; average normalized peak power =  $187.0 \pm 8.2$ ;  $n=3$ ; Figure 3c), indicating that anoctamin-1 does not contribute to the cycling of  $[Cl^-]_i$  in SCN neurons.

SCN neurons display a circadian rhythm in action potential firing frequency with a peak in the middle of the day (Inouye and Kawamura, 1979; Green and Gillette, 1982). Therefore, we next tested whether the observed rhythmicity in  $R_{Cl}$  may be dependent on action potential discharge—indeed, both  $R_{Cl}$  and SCN firing frequency share a similar phase, peaking around mid-day. However, when culturing SCN slices from AVP::Cl-Sensor mice in 2  $\mu$ M tetrodotoxin (TTX) to block voltage-dependent  $Na^+$  channels and action potential generation,  $R_{Cl}$  rhythmicity persisted (average period =  $23.3 \pm 0.2$  h; average normalized peak power =  $181.0 \pm 12.9$ ;  $n=4$  slices; Figure 4a). Therefore,  $R_{Cl}$  rhythmicity is not dependent on action potential generation. Although insensitive to TTX, it remained possible that  $R_{Cl}$  rhythmicity reflected the cycling of other voltage-dependent currents. In the SCN, a nimodipine-sensitive fast-oscillating calcium current has been identified in the presence of TTX (Jiang et al., 1997; Pennartz et al., 2002). To determine whether this  $Ca^{2+}$  current could regulate the  $R_{Cl}$  rhythm, we applied nimodipine (5  $\mu$ M) together with TTX. However, rhythmicity persisted in the presence of nimodipine (average period =  $23.0 \pm 0.3$  h; average normalized peak power =  $182.4 \pm 20.0$ ;  $n=3$  slices; Figure 4b). Together, these results indicate that  $R_{Cl}$  rhythmicity is independent of SCN excitability.

Activation of GABA<sub>A</sub> receptors produces localized increases of  $[Cl^-]_i$  that can alter the  $Cl^-$  equilibrium potential (Kuner and Augustine, 2000; Jedlicka et al., 2011). In the SCN, GABA activates synaptic GABA<sub>A</sub> receptors and is known to act at highly sensitive and

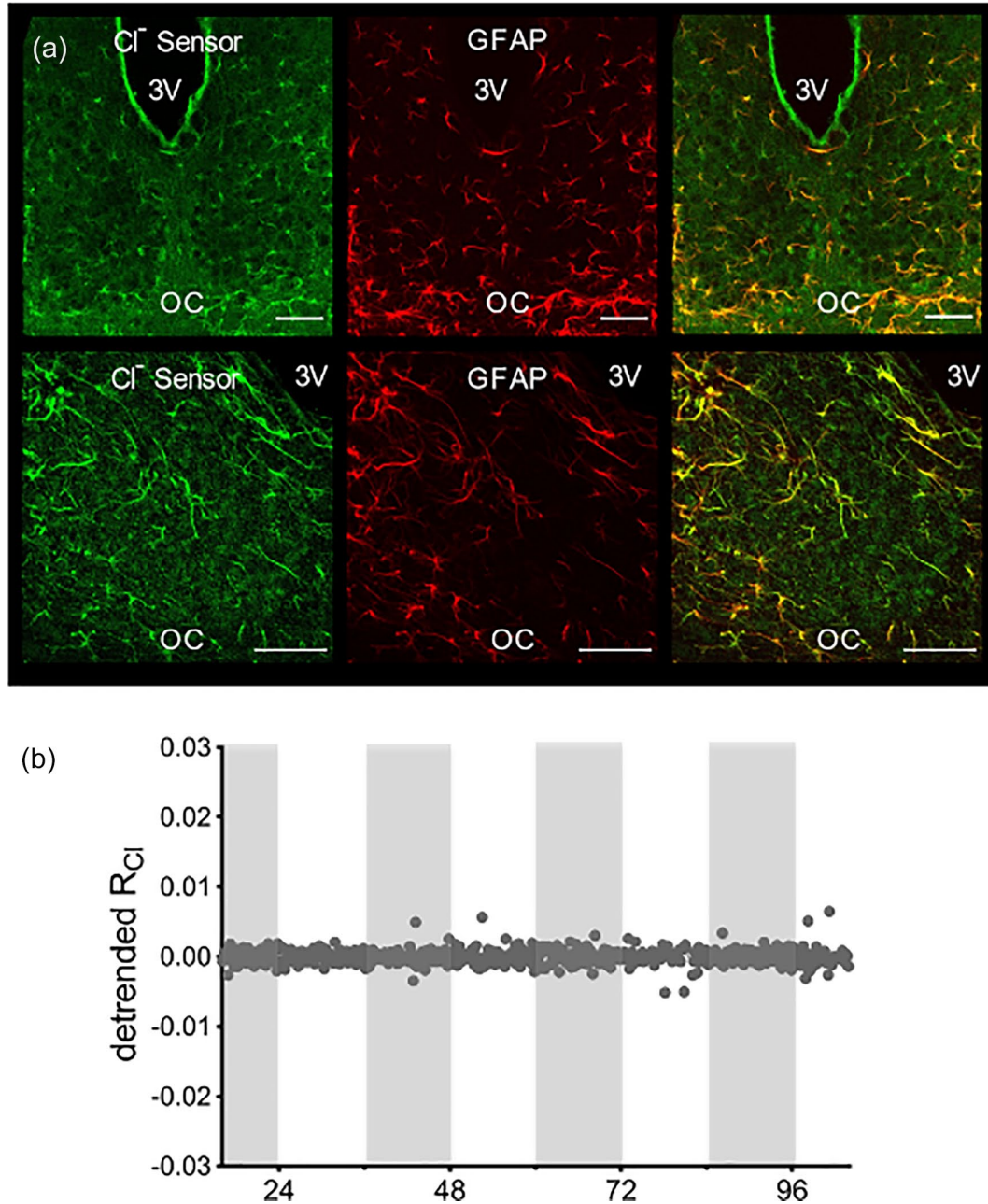


**Figure 2.**  $R_{Cl}$  does not cycle in GFAP + SCN astrocytes. (a) Confocal micrograph of the SCN from a GFAP::Cl-Sensor mouse. Native Cl-Sensor YFP fluorescence (left), GFAP immunostaining (center), and composite image (right). Top row: 20X; bottom row 40X. The scale bar indicates 50  $\mu$ m in all images. (b) Long-term imaging of  $R_{Cl}$  from a GFAP::Cl-Sensor mouse. Abbreviations:  $R_{Cl}$ =chloride ratio; GFAP=glial fibrillary acidic protein; SCN=suprachiasmatic nucleus; YFP=Yellow Fluorescent Protein; OC=Optic chiasm.

slowly desensitizing extrasynaptic GABA<sub>A</sub> receptors to produce a tonic GABA current (Moldavan et al., 2017; Moldavan et al., 2021; Brickley and Mody, 2012). To test if GABA transmission contributes to  $R_{Cl}$  oscillations, we cultured AVP::Cl-Sensor SCN slices in the presence of the GABA<sub>A</sub> receptor antagonists GABAzine and picrotoxin.  $R_{Cl}$  rhythmicity was detected in 7 of 8 GABAzine-treated slices and 4 of 7

picrotoxin-treated slices (Figure 5a and 5b). After excluding the non-rhythmic GABAzine and picrotoxin experiments, the remaining rhythmic trials demonstrated reduced normalized peak power in the Lomb-Scargle periodogram (GABAzine average:  $125.5 \pm 20.2$ ,  $n=7$ ; picrotoxin average:  $110.7 \pm 10.8$ ,  $n=4$ ) compared to control ( $184.9 \pm 7.3$ ,  $n=8$ , ANOVA:  $p < 0.0001$ , multiple comparisons:  $p = 0.0053$  for

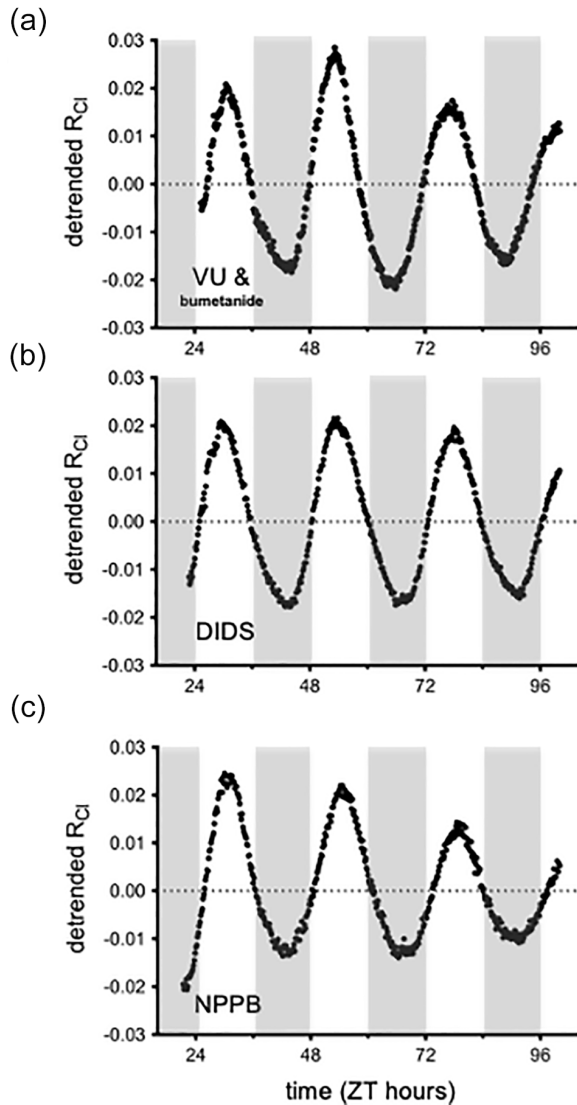


**Figure 3.**  $R_{Cl}$  rhythmicity persisted in the presence of antagonists to likely  $[Cl^-]$  regulators. Long-term imaging of  $R_{Cl}$  from an AVP::Cl-Sensor mouse cultured in the presence of either 100  $\mu M$  of the non-selective CCC blocker bumetanide and 20  $\mu M$  of the KCC antagonist VU0240551 (a), 100  $\mu M$  of the anion exchange inhibitor DIDS (b), or 20  $\mu M$  of the  $Cl^-$  channel blocker NPPB (c). Abbreviations:  $R_{Cl}$ =chloride ratio; AVP=arginine vasopressin; CCC=cation chloride cotransporter; KCC=potassium-chloride cotransporters; DIDS=4,4'-Diisothiocyano-2,2'-stilbenedisulfonic acid; NPPB=5-Nitro-2-(3-phenylpropylamino)benzoic acid; ZT=zeitgeber time.

GABA<sub>A</sub> and  $p=0.0029$  for picrotoxin, Figure 6d), indicating a reduction in rhythm strength (Figure 5b and 5d). Importantly, these results suggest that GABA<sub>A</sub> receptor signaling contributes to  $R_{Cl}$  rhythmicity. Because GABA<sub>A</sub> receptors are permeable to  $Cl^-$  ions,  $R_{Cl}$  rhythmicity may be a direct effect of  $Cl^-$  flux through GABA<sub>A</sub> receptors. Since Gabazine and picrotoxin were able to disrupt  $R_{Cl}$  rhythmicity, we

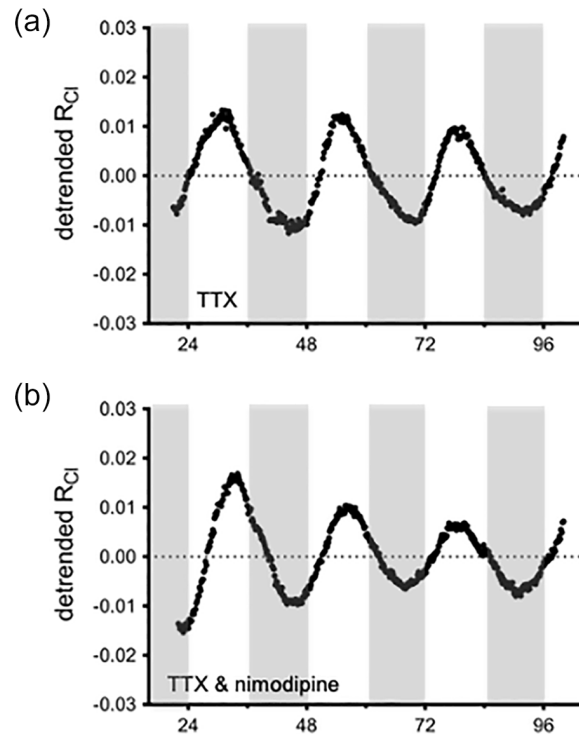


**Figure 4.**  $R_{Cl}$  rhythmicity is independent of action potential firing and calcium current activity. Long-term imaging of  $R_{Cl}$  from an AVP::Cl-Sensor mouse cultured in the presence of either 2  $\mu M$  TTX (a) or 2  $\mu M$  TTX with 5  $\mu M$  nimodipine (b). Abbreviations:  $R_{Cl}$ =chloride ratio; AVP=arginine vasopressin; TTX=Tetrodotoxin.

next asked if benzodiazepines are able to increase the rhythm's strength. Benzodiazepines are positive allosteric modulators of the GABA<sub>A</sub> receptor, so diazepam and zolpidem might be expected to increase rhythm strength or  $R_{Cl}$  amplitude by increasing  $Cl^-$  flux through GABA<sub>A</sub> receptors. However, when cultured in the presence of diazepam (5  $\mu M$ ) or zolpidem (10  $\mu M$ ), we found no effect of these drugs on either the amplitude of  $R_{Cl}$  itself or the rhythm strength (diazepam: average period =  $24.4 \pm 0.2$  h; average normalized peak power =  $218.2 \pm 2.7$ ;  $n=3$  slices; Figure 5e and 5f, zolpidem: average period =  $24.6 \pm 0.5$  h; average normalized peak power =  $217.6 \pm 6.4$ ;  $n=3$  slices; data not shown).

Like GABA receptors, glycine receptors allow for  $Cl^-$  flux through cell membranes. Indeed, glycine receptors have been described in the SCN (Ito et al., 1991; Prosser et al., 2008; Shinohara et al., 1998; Mordel et al., 2011). To test if glycine receptors contribute to  $R_{Cl}$  rhythmicity, we cultured SCN slices from AVP::Cl-Sensor mice in the presence of the glycine receptor antagonist strychnine. Strychnine did not prevent  $R_{Cl}$  from cycling or affect the strength of  $R_{Cl}$  rhythmicity (average period =  $26.1 \pm 1.1$  h; average normalized peak power =  $167.6 \pm 11.5$ ;  $n=3$ ; Figure 5g and 5h).



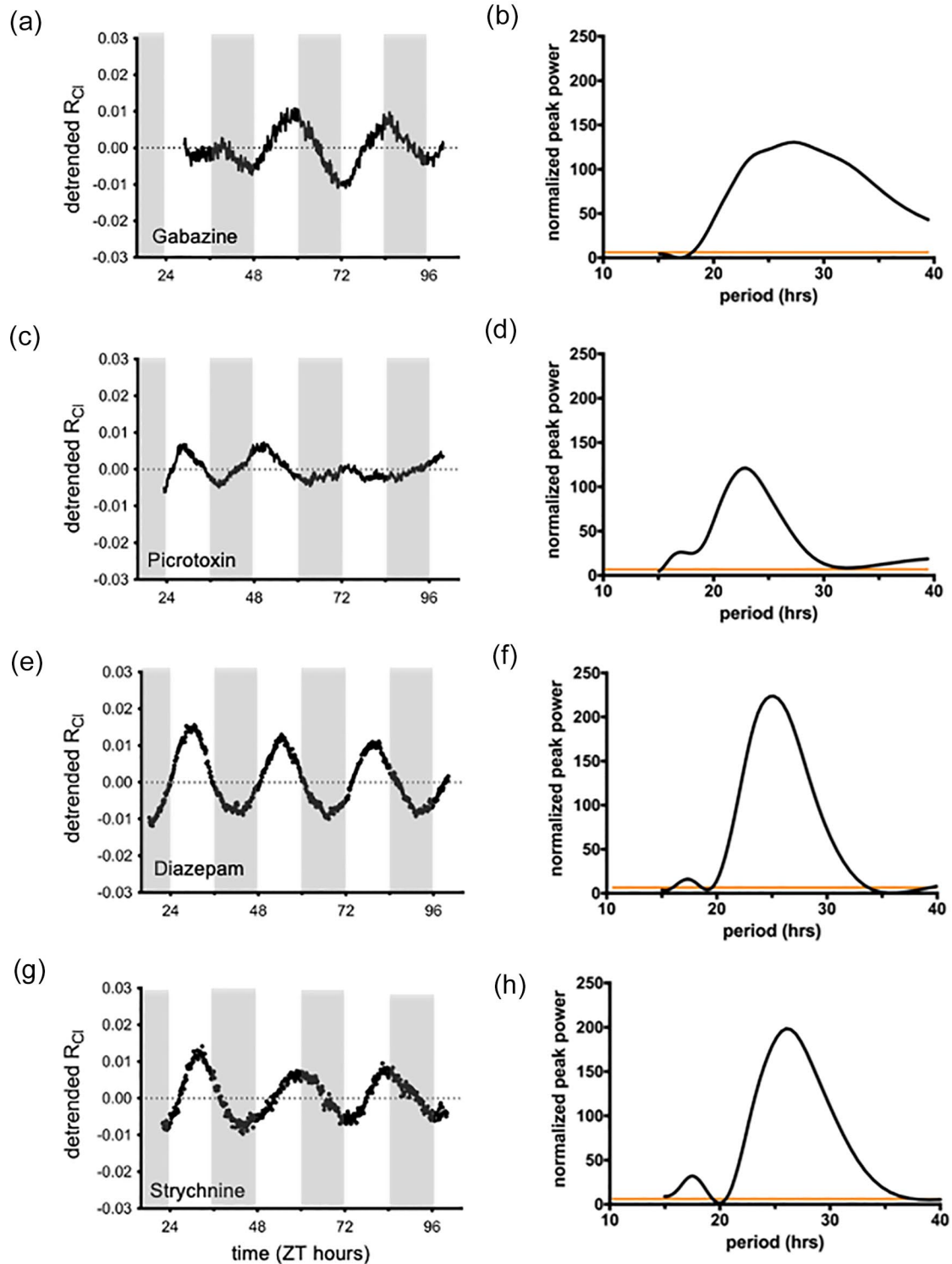
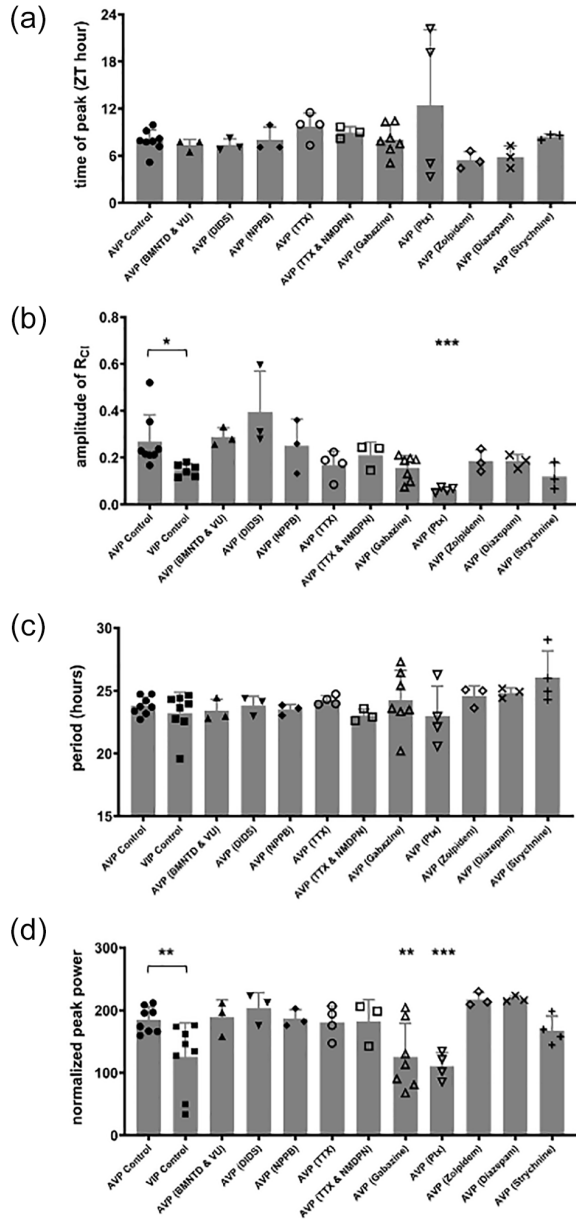


Figure 5. GABA neurotransmission contributes to  $R_{Cl}$  rhythmicity. Long-term imaging of  $R_{Cl}$  (left column) and Lomb-Scargle periodogram analysis (right column) from an AVP::Cl-Sensor mouse cultured in the presence of either 10  $\mu$ M GABazine (a, b) or 100  $\mu$ M picrotoxin (c, d). Although some experiments with GABA antagonists remained rhythmic, on average GABazine and picrotoxin experiments demonstrated a lower normalized peak power in periodogram analysis. Experiments with either 5  $\mu$ M diazepam (e, f) or 50  $\mu$ M strychnine (g, h). Abbreviations:  $R_{Cl}$  = chloride ratio; AVP = arginine vasopressin; ZT = zeitgeber time; GABA = gamma-aminobutyric acid.

## DISCUSSION



**Figure 6.** Summary of rhythm parameters across conditions. Time of peak (a) and amplitude of the first peak (b) obtained from a sine-wave fit of the detrended  $R_{Cl}$  trace. VIP::Cl-Sensor slices had a lower amplitude of  $R_{Cl}$  compared to AVP::Cl-Sensor slices (Student's *t*-test,  $p=0.03$ ). ANOVA analysis of  $R_{Cl}$  amplitude on AVP experiments revealed an effect of drug ( $p=0.0008$ ), with a post hoc multiple comparisons test yielding  $p=0.0031$  for picrotoxin. Period (c) and normalized peak power (d) from Lomb-Scargle periodogram analysis. VIP::Cl-Sensor slices had a lower normalized peak power compared to AVP::Cl-Sensor slices (Student's *t*-test,  $p=0.0121$ ). ANOVA analysis of power on AVP experiments revealed an effect of drug ( $p<0.0001$ ), with a post hoc multiple comparisons tests yielding  $p=0.0053$  for GABAazine and  $p=0.0029$  for picrotoxin. Abbreviations:  $R_{Cl}$ =chloride ratio; VIP=vasoactive intestinal peptide; AVP=arginine vasopressin; ZT=zeitgeber time; DIDS=4,4'-Diisothiocyanato-2,2'-stilbenedisulfonic acid; NPPB=5-Nitro-2-(3-phenylpropylamino)benzoic acid; TTX, Tetrodotoxin. BMNTD = Bumetanide; NMDPN=Nimodipine; VU=VU0240551; \* $p<0.05$ ; \*\* $p<0.01$ ; \*\*\* $p<0.005$

We observed that  $[Cl^-]_i$  oscillates in AVP + and VIP + neurons of the SCN. While other groups have suggested that  $[Cl^-]_i$  cycles in the SCN using estimates of the GABAergic reversal potential or observations of GABA-mediated excitation, we have directly assessed  $[Cl^-]_i$  using ratiometric imaging in genetically defined subpopulations of SCN neurons. We found that  $R_{Cl}$  peaked between ZT 7 and ZT 8 in AVP + and VIP + SCN neurons. The increased  $[Cl^-]_i$  will shift the  $[Cl^-]_i$  equilibrium potential to more positive voltages and increase the likelihood of an excitatory GABA response. This observation may provide a physiological basis for reports that have observed increased excitatory GABA transmission during the day and early night (Wagner et al., 1997; Albus et al., 2005; Choi et al., 2008; Irwin and Allen, 2009; Alamilla et al., 2014). In addition to neurotransmission,  $[Cl^-]_i$  is an important parameter involved in many cellular processes including pH regulation, cell volume regulation, and even membrane potential. Therefore, our observation of  $R_{Cl}$  rhythmicity offers important new insights into SCN physiology.

Although the Cl-Sensor transgene may be subject to the general rhythms of protein translation present in the SCN (Shibata et al., 1992; Chiang et al., 2014; Cao et al., 2011), the fact that Cl-Sensor is ratiometric, and therefore normalizes the Cl-sensitive YFP fluorescent signal to that of the Cl-insensitive CFP fluorescent signal, precludes the possibility that the observed rhythmicity in  $R_{Cl}$  reflects a rhythm in protein translation. Furthermore, we observed no rhythmicity in  $R_{Cl}$  when measured in GFAP + SCN astrocytes, indicating that the rhythmicity is specific to neurons, and does not represent an artifact of protein translation.

Methodological differences may explain the divergence of our  $[Cl^-]_i$  cycling observations from a report by DeWoskin et al. (2015), who observed no cycling  $[Cl^-]_i$  using the chloride indicator MQAE in SCN neurons. DeWoskin et al. loaded the entire SCN (including astrocytes) with the MQAE dye—therefore  $[Cl^-]_i$  rhythmicity in distinct subpopulations of SCN neurons (such as AVP +) may have been lost in the signal-to-noise ratio. Indeed, we did not observe  $R_{Cl}$  rhythmicity in GFAP + astrocytes. It is also worth noting that MQAE is not ratiometric, and therefore not well-equipped to normalize for artifacts related to dye concentration, fluorophore bleaching, tissue thickness, and dye leakage, which could potentially obscure rhythmicity in the MQAE signal (Arosio and Ratto, 2014).

Cl-Sensor is sensitive to protons in addition to the  $Cl^-$  ion (Markova et al., 2008), leaving open the possibility that the cycling of the fluorescent emission

signal ( $R_{Cl}$ ) could be attributed to circadian changes in pH. However, at low  $[Cl^-]_i$  (below 25 mM), an error in  $R_{Cl}$  measurements produced by pH changes is expected to be modest (Arosio and Ratto, 2014). Furthermore, intracellular pH is a tightly controlled physiological parameter, and pH homeostasis is essential to the proper functioning of a myriad of cellular processes. Therefore, we consider it unlikely that intracellular pH would vary with a circadian rhythm. Still, it remains possible that the rhythmicity of  $R_{Cl}$  could be affected by cycling of intracellular pH. This issue could be further addressed with the use of ClopHensorN, a genetically-encoded  $Cl^-$  indicator which is able to measure  $[Cl^-]_i$  and  $pH_i$  simultaneously (Arosio et al., 2010; Raimondo et al., 2013).

We observed that  $R_{Cl}$  amplitude and rhythm strength was larger in AVP::Cl-Sensor slices compared to VIP::Cl-Sensor SCN slices. Interestingly, this difference corresponds to the rhythmic expression of clock genes. Rhythmicity of *Per1* and *Per2* was observed in the dorsomedial shell of the SCN, but was absent, or of reduced amplitude, in the ventrolateral core (Hamada et al., 2001; Yan and Okamura, 2002; Hamada et al., 2004). Therefore, the observed rhythm in  $R_{Cl}$  may provide insight into the link between the molecular clock and SCN network physiology.

Several CCCs are expressed in the SCN (Kanaka et al., 2001; Belenky et al., 2008, 2010), and a functional contribution for these transporters in regulating  $[Cl^-]_i$  has been demonstrated (Choi et al., 2008; Irwin and Allen, 2009; Alamilla et al., 2014; Farajnia et al., 2014; Klett and Allen, 2017; Alamilla et al., 2014; Rohr et al., 2019; Myung et al., 2015; McNeill et al., 2018; Olde Engberink et al., 2018). Indeed, by imaging Cl-Sensor in acute SCN slices, we have previously demonstrated that  $R_{Cl}$  in AVP + and VIP + neurons responds to VU and bumetanide (Klett and Allen, 2017). However, we were not able to block  $R_{Cl}$  rhythmicity with these antagonists to the CCCs. Aside from the CCCs, neurons routinely express homeostatic regulators of  $[Cl^-]_i$ , such as the anion exchangers (Romero et al., 2004; Blaesse et al., 2009), but  $R_{Cl}$  rhythmicity persisted when targeting these transporters with the antagonist DIDS. In addition to transporters and ATP-dependent  $Cl^-$  pumps (Inoue et al., 1991), several chloride channels are expressed in the mammalian brain including the voltage-gated chloride channels (the ClC family), volume-regulated anion channel (VRACs), and the calcium-activated chloride channels (the CaCCs or anoctamins) (Jentsch and Pusch, 2018; Rahmati et al., 2018; Voss et al., 2014; Qiu et al., 2014). Indeed, the expression of anoctamin-1 has recently been demonstrated in the SCN, although its function has not been described (Aguilar-Roblero et al., 2018). We were not able to block  $R_{Cl}$  rhythmicity with the general blocker of  $Cl^-$  conductance, NPPB. Still,

neuronal  $Cl^-$  regulation is a relatively understudied and developing field (Duran et al., 2010), leaving open the possibility that other membrane proteins contribute to  $R_{Cl}$  rhythmicity in the SCN.

The  $R_{Cl}$  peak between ZT 7 and ZT 8 corresponds to the peak of action potential firing frequency (Inouye and Kawamura, 1979; Green and Gillette, 1982). Indeed, an increase in  $[Cl^-]_i$ , along with the concomitant increase in GABAergic excitation may contribute to the rise in action potential generation during the day. Although  $R_{Cl}$  oscillations may contribute to the rhythmic discharge of the SCN, action potentials are not necessary to generate the rhythm, as the cycling in  $R_{Cl}$  was not blocked by TTX. This finding is reminiscent to that observed for cytosolic  $Ca^{2+}$ , which was found to cycle independently of firing, and suggests that  $[Cl^-]_i$  may be under control of the molecular clock (Ikeda et al., 2003). However, Ikeda et al. observed cytosolic  $Ca^{2+}$  to peak at approximately CT 1.6 which precedes the peak of  $R_{Cl}$ , implying that these two signals are not directly linked.

Chloride influx through GABA<sub>A</sub> receptors is sufficient to drive changes in  $[Cl^-]_i$  (Jedlicka et al., 2011), therefore it is possible that GABA receptor activity underlies  $R_{Cl}$  rhythmicity. Indeed, the sensitivity of  $R_{Cl}$  to Gabazine and picrotoxin suggests that it is mediated, in part, by  $Cl^-$  fluxes through GABA<sub>A</sub> receptors. The frequency of spontaneous GABA currents (sIPSCs) oscillates in the dorsal SCN (Itri et al., 2004). However, the rhythmicity of sIPSCs was TTX-sensitive and peaked at ZT 12, while TTX had no effect on the rhythm of  $R_{Cl}$ . These observations suggest that the activation of synaptic GABA<sub>A</sub> receptors may not contribute to the rhythm in  $[Cl^-]_i$  that we observed. Alternatively, the activation of extrasynaptic GABA<sub>A</sub> receptors may underlie  $R_{Cl}$  rhythmicity. Indeed, extrasynaptic GABA receptors are known to be insensitive to benzodiazepines, and we found that  $R_{Cl}$  amplitude and rhythm strength were unchanged with either diazepam or zolpidem (Semyanov et al., 2004; Santhakumar et al., 2006). The first suggestion for the presence of a tonic GABA current in the SCN came from the observation of GAD67 expression in the SCN (Gao and Moore, 1996; Feldblum et al., 1993). Due to the lack of desensitization of GABA-induced currents in SCN neurons, Wagner et al. proposed that extrasynaptic GABA<sub>A</sub> receptors drive circadian changes in  $[Cl^-]_i$  (Wagner et al., 2001). More recently, a Gabazine-sensitive tonic GABA current has been directly measured in the SCN (Moldavan et al., 2017; Moldavan et al., 2021); however, the source of the GABA driving this current has not been identified. Ambient GABA levels in the extracellular fluid mediate the excitation of extrasynaptic GABA<sub>A</sub> receptors. Both vesicular and non-vesicular GABA sources contribute to the ambient GABA concentration. Non-vesicular GABA sources include extrusion

of GABA by GABA transporters (from both neurons and astrocytes) and permeation through bestrophin channels (Brickley and Mody, 2012). Although extracellular GABA concentrations in the SCN have not yet been directly measured across 24 h, biochemical methods have demonstrated that GABA levels in the entire hypothalamus show a circadian rhythm, with one study showing a peak during the day (Cattabeni et al., 1978; Aguilar-Roblero et al., 1993). Interestingly, vesicular release from dendrites has been demonstrated in the SCN (Castel et al., 1996), suggesting that dendritic GABA release could contribute to ambient GABA levels. Alternatively, astrocytes may contribute to ambient GABA levels in the SCN. Interestingly, Barca-Mayo et al. observed that GABA signaling from astrocytes was sufficient to rescue disrupted molecular rhythms in SCN neurons (Barca-Mayo et al., 2017). Although the source of GABA driving the tonic GABA current remains unclear, we propose that circadian changes in the ambient GABA concentration produce concurrent changes in the degree of extrasynaptic GABA<sub>A</sub> receptor activation to drive the rhythm in  $R_{Cl}$  observed in this study.

Because SCN neurons provide extensive local GABAergic innervation within the SCN (Freeman et al., 2013; Fan et al., 2015), our observation of rhythmic  $[Cl^-]_i$  provides important new insights into the circadian physiology of the SCN. We did not observe rhythmicity of  $R_{Cl}$  in GFAP + astrocytes, suggesting that  $R_{Cl}$  rhythmicity is specific to SCN neurons. Therefore, it would be interesting to determine if  $R_{Cl}$  rhythmicity is present in other types of SCN neurons. Indeed, several other Cre lines have been used in the SCN (Jones et al., 2015; Lee et al., 2015). Crossing such Cre lines with the floxed Cl-Sensor mouse used in this study would allow measurement of  $R_{Cl}$  in different and potentially larger populations of SCN neurons.



## ACKNOWLEDGMENTS

We thank Dr. Piotr Bregestovski for kindly providing us with the Cre-inducible Rosa26::Cl-Sensor mice. The authors disclose receipt of the following financial support for the research, authorship, and/or publication of this article: This work was supported by National Institutes of Health Grants NS036607 and NS103842 (CNA).

## CONFLICT OF INTEREST STATEMENT

The author(s) have no potential conflicts of interest with respect to the research, authorship, and/or publication of this article.

## ORCID iDs

Nathan J. Klett  <https://orcid.org/0000-0002-7102-1728>  
Charles N. Allen  <https://orcid.org/0000-0002-3689-2878>

## REFERENCES

- Aguilar-Roblero R, Mejia-Lopez A, Cortes-Pedroza D, Chavez-Juarez JL, Gutierrez-Monreal MA, Dominguez G, Vergara P, and Segovia J (2018) Calcium-regulated chloride channel anoctamin-1 is present in the suprachiasmatic nuclei of rats. *Neuroreport* 29:334-339.
- Aguilar-Roblero R, Verduzco-Carbajal L, Rodríguez C, Mendez-Franco J, Morán J, and Perez de la Mora M (1993) Circadian rhythmicity in the GABAergic system in the suprachiasmatic nuclei of the rat. *Neurosci Lett* 157:199-202.
- Alamilla J, Perez-Burgos A, Quinto D, and Aguilar-Roblero R (2014) Circadian modulation of the  $Cl^-$  equilibrium potential in the rat suprachiasmatic nuclei. *BioMed Res Int* 2014:424982.
- Albus H, Vansteensel MJ, Michel S, Block GD, and Meijer JH (2005) A GABAergic mechanism is necessary for coupling dissociable ventral and dorsal regional oscillators within the circadian clock. *Curr Biol* 15:886-893.
- Arosio D and Ratto GM (2014) Twenty years of fluorescence imaging of intracellular chloride. *Front Cell Neurosci* 8:258.
- Arosio D, Ricci F, Marchetti L, Gualdani R, Albertazzi L, and Beltram F (2010) Simultaneous intracellular chloride and pH measurements using a GFP-based sensor. *Nature Methods* 7:516-518.
- Barca-Mayo OM, Pons-Espinal MP, Follert PA, Armirotti AL, Berdondini L, and De Pietri Tonelli D (2017) Astrocyte deletion of Bmal1 alters daily locomotor activity and cognitive functions via GABA signalling. *Nat Commun* 8:14336.
- Batti L, Mukhtarov M, Audero E, Ivanov A, Paolicelli O, Zurborg S, Gross C, Bregestovski P, and Heppenstall PA (2013) Transgenic mouse lines for non-invasive ratiometric monitoring of intracellular chloride. *Front Mol Neurosci* 6:11.
- Belenky MA, Sollars PJ, Mount DB, Alper SL, Yarom Y, and Pickard GE (2010) Cell-type specific distribution of chloride transporters in the rat suprachiasmatic nucleus. *Neuroscience* 165:1519-1537.
- Belenky MA, Yarom Y, and Pickard GE (2008) Heterogeneous expression of gamma-aminobutyric acid and gamma-aminobutyric acid-associated receptors and transporters in the rat suprachiasmatic nucleus. *J Comp Neurol* 506:708-732.
- Ben-Ari Y, Woodin MA, Sernagor E, Cancedda L, Vinay L, Rivera C, Legendre P, Luhmann HJ, Bordey A, Wennner P, et al. (2012) Refuting the challenges of the developmental shift of polarity of GABA actions: GABA more exciting than ever!. *Front Cell Neurosci* 6:35.



- Berg J, Yang H, and Jan LY (2012) Ca<sup>2+</sup>-activated Cl<sup>-</sup> channels at a glance. *J Cell Sci* 125:1367-1371.
- Blaesse P, Airaksinen MS, Rivera C, and Kaila K (2009) Cation-chloride cotransporters and neuronal function. *Neuron* 61:820-838.
- Brickley SG and Mody I (2012) Extrasynaptic GABA(A) receptors: their function in the CNS and implications for disease. *Neuron* 73:23-34.
- Cao R, Anderson FE, Jung YJ, Dziema H, and Obrietan K (2011) Circadian regulation of mammalian target of rapamycin signaling in the mouse suprachiasmatic nucleus. *Neuroscience* 181:79-88.
- Castel M, Morris J, and Belenky M (1996) Non-synaptic and dendritic exocytosis from dense-cored vesicles in the suprachiasmatic nucleus. *Neuroreport* 7:543-547.
- Cattabeni F, Maggi A, Monduzzi M, De Angelis L, and Racagni G (1978) GABA: circadian fluctuations in rat hypothalamus. *J Neurochem* 31:565-567.
- Chiang CK, Mehta N, Patel A, Zhang P, Ning Z, Mayne J, Sun WY, Cheng HY, and Figeys D (2014) The proteomic landscape of the suprachiasmatic nucleus clock reveals large-scale coordination of key biological processes. *PLoS Genet* 10:e1004695.
- Choi HJ, Lee CJ, Schroeder A, Kim YS, Jung SH, Kim JS, Kim do Y, Son EJ, Han HC, Hong SK, et al. (2008) Excitatory actions of GABA in the suprachiasmatic nucleus. *J Neurosci* 28:5450-5459.
- De Jeu M and Pennartz CMA (2002) Circadian modulation of GABA function in the rat suprachiasmatic nucleus: excitatory effects during the night phase. *J Neurophysiol* 87:834-844.
- Delpire E, Days E, Lewis LM, Mi D, Kim K, Lindsley CW, and Weaver CD (2009) Small-molecule screen identifies inhibitors of the neuronal K-Cl cotransporter KCC2. *Proc Natl Acad Sci USA* 106:5383-5388.
- DeWoskin D, Myung J, Belle MD, Piggins HD, Takumi T, and Forger DB (2015) Distinct roles for GABA across multiple timescales in mammalian circadian timekeeping. *Proc Natl Acad Sci USA* 112:E3911-3919.
- Duran C, Thompson CH, Xiao Q, and Hartzell HC (2010) Chloride channels: often enigmatic, rarely predictable. *Ann Rev Physiol* 72:95-121.
- Evans JA, Leise TL, Castanon-Cervantes O, and Davidson AJ (2013) Dynamic interactions mediated by nonredundant signaling mechanisms couple circadian clock neurons. *Neuron* 80:973-983.
- Fan J, Zeng H, Olson DP, Huber KM, Gibson JR, and Takahashi JS (2015) Vasoactive intestinal polypeptide (VIP)-expressing neurons in the suprachiasmatic nucleus provide sparse GABAergic outputs to local neurons with circadian regulation occurring distal to the opening of postsynaptic GABAA ionotropic receptors. *J Neurosci* 35:1905-1920.
- Farajnia S, van Westering TL, Meijer JH, and Michel S (2014) Seasonal induction of GABAergic excitation in the central mammalian clock. *Proc Natl Acad Sci USA* 111:9627-9632.
- Farrant M and Kaila K (2007) The cellular, molecular and ionic basis of GABA(A) receptor signalling. *Prog Brain Res* 160:59-87.
- Feldblum S, Erlander MG, and Tobin AJ (1993) Different distributions of GAD65 and GAD67 mRNAs suggest that the two glutamate decarboxylases play distinctive functional roles. *J Neurosci Res* 34:689-706.
- Freeman GM Jr, Krock RM, Aton SJ, Thaben P, and Herzog ED (2013) GABA networks destabilize genetic oscillations in the circadian pacemaker. *Neuron* 78:799-806.
- Friedel P, Bregestovski P, and Medina I (2013) Improved method for efficient imaging of intracellular Cl<sup>-</sup> with Cl-Sensor using conventional fluorescence setup. *Front Mol Neurosci* 6:7.
- Gamba G (2005) Molecular physiology and pathophysiology of electroneutral cation-chloride cotransporters. *Physiol Rev* 85:423-493.
- Gao B and Moore RY (1996) Glutamic acid decarboxylase message isoforms in human suprachiasmatic nucleus. *J Biol Rhythm* 11:172-179.
- Gillespie CF, Huhman KL, Babagbemi TO, and Albers HE (1996) Bicuculline increases and muscimol reduces the phase-delaying effects of light and VIP/PHI/GRP in the suprachiasmatic region. *J Biological Rhythm* 11:137-144.
- Gillespie CF, Mintz EM, Marvel CL, Huhman KL, and Albers HE (1997) GABAA and GABAB agonists and antagonists alter the phase-shifting effects of light when microinjected into the suprachiasmatic region. *Brain Res* 759:181-189.
- Green DJ and Gillette R (1982) Circadian rhythm of firing rate recorded from single cells in the rat suprachiasmatic brain slice. *Brain Res* 245:198-200.
- Hablitz LM, Gunesch AN, Cravetich O, Moldavan M, and Allen CN (2020) Cannabinoid signaling recruits astrocytes to modulate presynaptic function in the suprachiasmatic nucleus. *eNeuro* 7(1):ENEURO.0081-19.2020.
- Hamada T, Antle MC, and Silver R (2004) Temporal and spatial expression patterns of canonical clock genes and clock-controlled genes in the suprachiasmatic nucleus. *Eur J Neurosci* 19:1741-1748.
- Hamada T, LeSauter J, Venuti JM, and Silver R (2001) Expression of Period genes: rhythmic and nonrhythmic compartments of the suprachiasmatic nucleus pacemaker. *J Neurosci* 21:7742-7750.
- Harris JA, Hirokawa KE, Sorensen SA, Gu H, Mills M, Ng LL, Bohn P, Mortrud M, Ouellette B, Kidney J, et al. (2014) Anatomical characterization of Cre driver mice for neural circuit mapping and manipulation. *Front Neural Circ* 8:76.
- Huang WC, Xiao S, Huang F, Harfe BD, Jan YN, and Jan LY (2012) Calcium-activated chloride channels (CaCCs) regulate action potential and synaptic response in hippocampal neurons. *Neuron* 74:179-192.
- Ikeda M, Sugiyama T, Wallace CS, Gompf HS, Yoshioka T, Miyawaki A, and Allen CN (2003) Circadian dynamics of cytosolic and nuclear Ca(2+) in single suprachiasmatic nucleus neurons. *Neuron* 38:253-263.

- Inoue M, Hara M, Zeng XT, Hirose T, Ohnishi S, Yasukura T, Uriu T, Omori K, Minato A, and Inagaki C (1991) An ATP-driven Cl<sup>-</sup> pump regulates Cl<sup>-</sup> concentrations in rat hippocampal neurons. *Neurosci Lett* 134:75-78.
- Inouye ST and Kawamura H (1979) Persistence of circadian rhythmicity in a mammalian hypothalamic "island" containing the suprachiasmatic nucleus. *Proc Natl Acad Sci USA* 76:5962-5966.
- Irwin RP and Allen CN (2009) GABAergic signaling induces divergent neuronal Ca(2+) responses in the suprachiasmatic nucleus network. *Eur J Neurosci* 30:1462-1475.
- Ito C, Wakamori M, and Akaike N (1991) Dual effect of glycine on isolated rat suprachiasmatic neurons. *Am J Physiol Cell Physiol* 260:C213-C218.
- Itri J, Michel S, Waschek JA, and Colwell CS (2004) Circadian rhythm in inhibitory synaptic transmission in the mouse suprachiasmatic nucleus. *J Neurophysiol* 92:311-319.
- Jedlicka P, Deller T, Gutkin BS, and Backus KH (2011) Activity-dependent intracellular chloride accumulation and diffusion controls GABA(A) receptor-mediated synaptic transmission. *Hippocampus* 21:885-898.
- Jentsch TJ and Pusch M (2018) CLC chloride channels and transporters: structure, function, physiology, and disease. *Physiol Rev* 98:1493-1590.
- Jeon JH, Paik SS, Chun MH, Oh U, and Kim IB (2013) Presynaptic localization and possible function of calcium-activated chloride channel anoctamin 1 in the mammalian retina. *PLoS ONE* 8:e67989.
- Jiang ZG, Yang YQ, and Allen CN (1997) Tracer and electrical coupling of rat suprachiasmatic nucleus neurons. *Neuroscience* 77:1059-1066.
- Jones JR, Tackenberg MC, and McMahon DG (2015) Manipulating circadian clock neuron firing rate resets molecular circadian rhythms and behavior. *Nat Neurosci* 18:373-375.
- Kanaka C, Ohno K, Okabe A, Kuriyama K, Itoh T, Fukuda A, and Sato K (2001) The differential expression patterns of messenger RNAs encoding K-Cl cotransporters (KCC1,2) and Na-K-2Cl cotransporter (NKCC1) in the rat nervous system. *Neuroscience* 104:933-946.
- Klett NJ and Allen CN (2017) Intracellular chloride regulation in AVP+ and VIP+ neurons of the suprachiasmatic nucleus. *Sci Rep* 7:10226.
- Kuner T and Augustine GJ (2000) A genetically encoded ratiometric indicator for chloride: capturing chloride transients in cultured hippocampal neurons. *Neuron* 27:447-459.
- Lee IT, Chang AS, Manandhar M, Shan Y, Fan J, Izumo M, Ikeda Y, Motoike T, Dixon S, Seinfeld JE, et al. (2015) Neuromedin s-producing neurons act as essential pacemakers in the suprachiasmatic nucleus to couple clock neurons and dictate circadian rhythms. *Neuron* 85:1086-1102.
- Liu C and Reppert SM (2000) GABA synchronizes clock cells within the suprachiasmatic circadian clock. *Neuron* 25:123-128.
- Markova O, Mukhtarov M, Real E, Jacob Y, and Bregestovski P (2008) Genetically encoded chloride indicator with improved sensitivity. *J Neurosci Methods* 170:67-76.
- McNeill JK, Walton JC, and Albers HE (2018) Functional significance of the excitatory effects of GABA in the suprachiasmatic nucleus. *J Biol Rhythms* 33:376-387.
- Moldavan MG, Cravetchi O, and Allen CN (2017) GABA transporters regulate tonic and synaptic GABA receptor-mediated currents in the suprachiasmatic nucleus neurons. *J Neurophysiol* 118:3092-3106.
- Moldavan M, Cravetchi O, and Allen CN (2021) Diurnal properties of tonic and synaptic GABA receptor-mediated currents in suprachiasmatic nucleus neurons. *J Neurophysiol* 126(2):637-652.
- Moldavan MG, Irwin RP, and Allen CN (2006) Presynaptic GABAB receptors regulate retinohypothalamic tract synaptic transmission by inhibiting voltage-gated Ca2+ channels. *J Neurophysiol* 95:3727-3741.
- Mordel J, Karnas D, Inyushkin A, Challet E, Pévet P, and Meissl H (2011) Activation of glycine receptor phase-shifts the circadian rhythm in neuronal activity in the mouse suprachiasmatic nucleus. *J Physiol* 589:2287-2300.
- Myung J, Hong S, DeWoskin D, De Schutter E, Forger DB, and Takumi T (2015) GABA-mediated repulsive coupling between circadian clock neurons in the SCN encodes seasonal time. *Proc Nat Acad Sci USA* 112:E3920-E3929.
- Olde Engberink AHO, Meijer JH, and Michel S (2018) Chloride cotransporter KCC2 is essential for GABAergic inhibition in the SCN. *Neuropharmacol* 138:80-86.
- Pennartz CMA, de Jeu MT, Bos NP, Schaap J, and Geurtsen AM (2002) Diurnal modulation of pacemaker potentials and calcium current in the mammalian circadian clock. *Nature* 416:286-290.
- Prosser RA, Mangrum CA, and Glass JD (2008) Acute ethanol modulates glutamatergic and serotonergic phase shifts of the mouse circadian clock in vitro. *Neuroscience* 152:837-848.
- Qiu Z, Dubin AE, Mathur J, Tu B, Reddy K, Miraglia LJ, Reinhardt J, Orth AP, and Patapoutian A (2014) SWELL1, a plasma membrane protein, is an essential component of volume-regulated anion channel. *Cell* 157:447-458.
- Rahmati N, Hoebeek FE, Peter S, and De Zeeuw CI (2018) Chloride homeostasis in neurons with special emphasis on the olivocerebellar system: differential roles for transporters and channels. *Front Cell Neurosci* 12:101.
- Raimondo JV, Joyce B, Kay L, Schlagheck T, Newey SE, Srinivas S, and Akerman CJ (2013) A genetically-encoded chloride and pH sensor for dissociating ion dynamics in the nervous system. *Front Cell Neurosci* 7:202.

- Rohr KE, Pancholi H, Haider S, Karow C, Modert D, Raddatz NJ, and Evans J (2019) Seasonal plasticity in GABAA signaling is necessary for restoring phase synchrony in the master circadian clock network. *eLife* 8:e49578.
- Romero MF, Fulton CM, and Boron WF (2004) The SLC4 family of HCO<sub>3</sub><sup>-</sup>—transporters. *Pflügers Arch* 447:495-509.
- Ruf T (1999) The Lomb-Scargle periodogram in biological rhythm research: analysis of incomplete and unequally spaced time-series. *Biol Rhythm Res* 30:178-201.
- Santhakumar V, Hancher HJ, Wallner M, Olsen RW, and Otis TS (2006) Contributions of the GABAA receptor  $\alpha 6$  subunit to phasic and tonic inhibition revealed by a naturally occurring polymorphism in the  $\alpha 6$  gene. *J Neurosci* 26:3357-3364.
- Semyanov A, Walker MC, Kullmann DM, and Silver RA (2004) Tonically active GABA(A) receptors: modulating gain and maintaining the tone. *Trends Neurosci* 27:262-269.
- Shibata S, Hamada T, Tominaga K, and Watanabe S (1992) An in vitro circadian rhythm of protein synthesis in the rat suprachiasmatic nucleus under tissue culture conditions. *Brain Res* 584:251-256.
- Shinohara K, Honma S, Katsuno Y, Abe H, and Honma K (1998) Circadian release of amino acids in the suprachiasmatic nucleus in vitro. *Neuroreport* 9:137-140.
- Sonoda T, Li JY, Hayes NW, Chan JC, Okabe Y, Belin S, Nawabi H, and Schmidt TM (2020) A noncanonical inhibitory circuit dampens behavioral sensitivity to light. *Science* 368:527-531.
- Taniguchi H, He M, Wu P, Kim S, Paik R, Sugino K, Kvitsani D, Fu Y, Lu J, Lin Y, et al. (2011) A resource of Cre driver lines for genetic targeting of GABAergic neurons in cerebral cortex. *Neuron* 71:995-1013.
- Valeeva G, Tressard T, Mukhtarov M, Baude A, and Khazipov R (2016) An optogenetic approach for investigation of excitatory and inhibitory network GABA actions in mice expressing channelrhodopsin-2 in GABAergic neurons. *J Neurosci* 36:5961-5973.
- van den Pol AN (1986) Gamma-aminobutyrate, gastrin releasing peptide, serotonin, somatostatin, and vasopressin: ultrastructural immunocytochemical localization in presynaptic axons in the suprachiasmatic nucleus. *Neuroscience* 17:643-659.
- Voss KF, Ullrich F, Munch J, Lazarow K, Lutter D, Mah N, Andrade-Navarro MA, von Kries JP, Stauber T, and Jentsch TJ (2014) Identification of LRRC8 heteromers as an essential component of the volume-regulated anion channel VRAC. *Science* 344:634-638.
- Wagner S, Castel M, Gainer H, and Yarom Y (1997) GABA in the mammalian suprachiasmatic nucleus and its role in diurnal rhythmicity. *Nature* 387:598-603.
- Wagner S, Sagiv N, and Yarom Y (2001) GABA-induced current and circadian regulation of chloride in neurons of the rat suprachiasmatic nucleus. *J Physiol* 537:853-869.
- Yan L and Okamura H (2002) Gradients in the circadian expression of *Per1* and *Per2* genes in the rat suprachiasmatic nucleus. *Eur J Neurosci* 15:1153-1162.